Original Article

The Inhibitory Effect of Camel Lactoferrin-chimera, a Recombinant Antimicrobial Peptide, on Avian Influenza Virus Subtype H9N2

Moein Khodayari[1] (ID), **Mohammad Hadi Sekhavati[2]** (ID), **Seyed Mostafa Peighambari[1]** (ID), **Abbas Barin[3]** (ID), **Omid Dezfoulian[4]** (ID), **Jamshid Razmyar[1*]** (ID)

1. Department of Avian Diseases, Faculty of Veterinary Medicine, University of Tehran, Tehran, Iran.
2. Department of Animal Science, Faculty of Agriculture, Ferdowsi University of Mashhad, Mashhad, Iran.
3. Department of Clinical Pathology, Faculty of Veterinary Medicine, University of Tehran, Tehran, Iran.
4. Department of Pathobiology, School of Veterinary Medicine, Lorestan University, Khorramabad, Iran.

ABSTRACT

Background: Avian influenza subtype H9N2 is poultry's most prevalent influenza virus worldwide. It imposes economic losses to the poultry industry and has zoonotic potential. Currently, the two main groups of anti-influenza drugs are adamantanes and neuraminidase inhibitors. In recent years, there has been an increase in the resistance to existing anti-influenza drugs. Antimicrobial peptides are a group of potential drug candidates with broad-spectrum activity. Camel lactoferrin (cLF)-chimera is an antimicrobial peptide synthesized from camel milk lactoferrin.

Objectives: This study aims to evaluate the inhibitory effects of cLF-chimera on avian influenza, subtype H9N2.

Methods: One hundred and seventy 11-day-old specific pathogen-free (SPF) embryonated eggs were randomly distributed into 17 groups. Different virus and peptide concentrations were injected into the eggs. The eggs were incubated for four days, and daily candling was done for viability assessment. On the 4th day of incubation, each group's live or dead embryos were sorted and evaluated for gross anomalies. Next, for histopathological analysis, chick embryos were fixed with 10% neutral buffered formalin for one week. The 3-(4,5-dimethylthiazol-2-yl)-2,5 diphenyl tetrazolium bromide (MTT) assay was performed to determine peptide and virus concentrations.

Results: Embryo viability results and macroscopic and histopathologic findings showed that the peptide had inhibitory effects against the virus. These results are consistent with the 3-(4,5-dimethylthiazol-2-yl)-2,5 diphenyl tetrazolium bromide) (MTT) assay. Moreover, the peptide has proven effects against pathogenic bacteria, which can be advantageous compared to common anti-influenza medications.

Conclusion: According to the results, cLF-chimera has an inhibitory effect on the H9N2 influenza virus

Keywords: Antimicrobial peptide, Avian influenza, Camel lactoferrin (cLF)-chimera, Histopathology, Subtype H9N2

* Corresponding Author:

Jamshid Razmyar, Associate Professor.

Address: Department of Avian Diseases, Faculty of Veterinary Medicine, University of Tehran, Tehran, Iran.

Phone: +98 (21) 66933222

E-mail: jrazmyar@ut.ac.ir

Introduction

Avian influenza viruses (AIVs) have a negative-sense ribonucleic acid (RNA) genome with eight segments in the Orthomyxoviridae family and Influenza A genus (Perez DR 2019, Mohammadi et al., 2023). They are categorized as high or low pathogenic based on their pathogenicity and molecular markers. They are also classified into 16 haemagglutinin (HA) and nine neuraminidase (NA) subtypes based on surface glycoproteins HA and NA (Swayne et al., 2020, Sheykhi et al., 2021). The H9N2 subtype is a low-pathogenic AIV (LPAIV), the most prevalent AIV in poultry worldwide (Nagyet al., 2017). Its first report was from turkeys in the USA in 1966 (Nagy et al., 2017). Later, it spread to Asia, especially in the 1990s (Nagy et al., 2017; Mehrabadi et al., 2019). The first report on H9N2 in Iran was by Vasfi et al. in 1998 (Vasfi Marandi et al., 2002). Since then, the virus has been endemic in Iran and reported frequently (Ahmadi et al., 2018).

H9N2 AIV is crucial for the following reasons: I: Due to direct and indirect economic losses, such as mortality, vaccination, and treatment costs (Swayne et al., 2020); II: Possible transmission to humans. The first zoonotic species was reported in China in 1998 (Peacock et al., 2019, Mayahi et al., 2021). Fortunately, it is sporadic with low severity in humans, and there have been no reports of transmission among the human population, but the virus can be considered a pandemic candidate (Pusch & Suarez, 2018). III: H9N2 is a gene donor. To date, the role of H9N2 AIV in the emergence of at least three influenza subtypes, H5N1 (Peacock et al., 2019), H7N9 (Lam et al., 2013), and H10N8 (Chen et al., 2014), has been recognized.

Poultry prevention strategies are based on vaccination and biosecurity (Shen et al., 2014, Radmehri et al., 2021, Motamedinasab et al., 2023). However, vaccination is the primary strategy, and its effectiveness is mainly influenced by the similarity between the vaccine and the virus HA glycoprotein (Song & Qin, 2020). In addition, vaccination of birds with immunosuppressive diseases has no optimal effect (Sharif & Ahmad, 2018).

In humans, anti-influenza drugs are used for treatment and prevention (Amarelle et al., 2017). The two main types of medicines, adamantanes and neuraminidase inhibitors have been proven in many countries (Koszalka et al., 2017). The mechanisms of action for these drugs are blocking the M2 ion channel and neuraminidase glycoprotein, respectively (Watanabe & Kawaoka, 2015).

Vaccination and biosecurity of poultry cannot completely prevent disease outbreaks. Currently, no specific treatment is found for poultry, and human anti-influenza drugs are prohibited in many countries (Tsuruoka et al., 2017; Ahmadi, Rajabi et al., 2018). In contrast, drug resistance, especially for adamantanes, has increased in recent years (Hussain et al., 2017). In addition, prescribing these drugs 48 h after the onset of symptoms is not considered effective (Lehnert et al., 2016). Therefore, it is required to search for new anti-influenza agents that can also be used in poultry, that antimicrobial peptides (AMPs) are one of many candidates (Ahmadi et al., 2018; De Angelis et al., 2021).

AMPs or host defense peptides are small amino acid molecules (usually <100) that are part of the innate immune system (Kang et al., 2017; Lei et al., 2019). These peptides exist in many organisms (Lei et al., 2019) and have a broad-spectrum effect on bacteria, fungi, and cancer cells (Yeaman & Yount, 2003, Ong et al,. 2014). Peptides are also acceptable candidates for preventing and treating viral diseases, with proven antiviral activity against some DNA and ribonucleic acid (RNA) viruses (Bahar & Ren, 2013).

A group of AMPs are derived from larger proteins. The N-terminus of lactoferrin contains hydrophobic and cationic AMPs with antibacterial, antiviral, and antifungal activities (Tanhaiean et al., 2018a, Tanhaieian et al., 2018b). The chimeric peptide camel lactoferrin (cLF)-chimera is derived from camel milk lactoferrin. The peptide is synthesized from the linkage of the camel lactoferricin (cLFcin) C-terminus and camel lactoferampin (cLFampin) N-terminus by a lysine amino acid (Tanhaiean et al., 2018a; Pirkhezranian et al., 2020) and expressed recombinantly in *Escherichia coli* and *L. lactis* (Tanhaiean et al., 2018a; Tanhaieiani et al., 2018b). The peptide had an antibacterial effect against *E. coli*, *S. Enteritidis*, *S. Typhi*, *P. aeruginosa*, and *S. aureus* in vitro and *E. coli* and *C. perfringens*, in vivo (Daneshmand et al., 2019; Daneshmand et al., 2020; Roshana et al., 2020, Tanhaeian et al., 2020).

Some natural and synthetic AMP studies have focused on antiviral drugs in humans and birds. However, most studies have concentrated on human pathogens, such as Middle East respiratory syndrome coronavirus (MERS-CoV), severe acute respiratory syndrome coronavirus 2 (SARS-CoV), human immunodeficiency virus (HIV), hepatitis C virus, and measles (Zhao et al., 2020), while others have focused on avian pathogens. One crucial potential zoonotic pathogen is AIV. Different peptides have been tested on different subtypes of AIV, such as H1, H3, H5, and H7 (Li et al., 2011; Zhao et al., 2016) and H9N2 (Rajik et al., 2009; Arbi et al., 2022).

In this study, we also decided to predict the interaction of the peptide with its partially related receptors (HA, NA, and M2 ion channels). To accomplish this, we used a computational modeling technique. Computational modeling has the benefits of reducing wet lab practice costs and minimizing blind experiments (Meng et al., 2011). On the other hand, molecular docking has been accepted as a modeling technique that could elucidate the interaction between molecules (Pagadala et al., 2017). This method explains the ligand and target protein's most favorable binding mode (Tripathi & Bankaitis, 2017). Therefore, it can be used in molecular biology and drug design (Meng et al., 2011, Pagadala et al., 2017).

This study was conducted to evaluate the probable inhibitory effects of cLFchimera on the H9N2 subtype of influenza virus to prevent and treat influenza in both humans and poultry. Moreover, computational modeling predicts the interaction between the peptide and the virus surface projections (HA, NA, M2).

Materials and Methods

Virus, cells, and embryonated eggs

Low-pathogenic AIV (LPAIV) strain A/chicken/Iran/UT-Barin/2017 (H9N2) was used in this study. The virus was obtained from the Department of Avian Diseases, Faculty of Veterinary Medicine, University of Tehran. Madin-Darby canine kidney (MDCK) cells were purchased from Razi Vaccine & Serum Research Institute, Iran, and maintained in Dulbecco's minimal essential medium (Thermo Fisher Scientific corporation; USA), with 10% fetal bovine serum (Thermo Fisher Scientific corporation; USA) at 37 centigrade degrees and 5% CO_2 atmosphere. Eleven-day-old specific pathogen-free (SPF) embryonated eggs were also used to evaluate possible virus-peptide interactions.

Camel lactoferrin (cLF)-chimera peptide

The chimeric peptide was derived from camel milk lactoferrin. It is synthesized from the linkage of the cLF-cin C-terminus (17-30) and the cLFampin N-terminus (265–284) by a lysine amino acid. A six-aminoacids-histidine tag is also linked to lactoferampin (Tanhaiean et al., 2018b, Tanhaieian et al., 2018b). Figure 1 shows the peptide's cartoon shape and amino acid sequence.

Experimental design

The study was conducted in six steps:

Titration of the virus by the embryo infective dose50 (EID50) method

First, a ten-fold dilution of the virus was prepared. Serial dilution continued to 10-9. Each dilution was injected into five SPF embryonated eggs. After incubation at 37 °C and 75% humidity for 72 h, the number of live and dead embryos in each group was counted. The CAF of all the eggs were then harvested. The presence of the virus in the fluids were evaluated using the HA test. To increase the accuracy, the HA test was performed in duplicate. The Reed and Muench method was performed to reach 102, 104, and 106 embryo infective dose 50 (EID50) of the virus (Villegas, 2008).

Injection of the peptide and titrated virus into embryonated eggs

Eleven-day-old SPF embryonated eggs were randomly divided into 17 groups (each with ten eggs). After peptide dilutions were prepared (40, 80, and 160 μg) (Torres et al., 2013, Tahmoorespur et al., 2020), 0.1 mL of each dilution was mixed with 0.1 mL of the virus dilutions (102, 104, and 106 EID50). The mixture was then remained at room temperature for 30 minutes. Then, each inoculum was injected into the allantoic sac of embryonated eggs (Tare & Pawar, 2015). There were three groups: Positive, negative, and injection control. Table 1 summarizes all treatment groups.

Evaluation of macroscopic and histopathologic lesions of the embryos

The eggs were incubated for four days (Arbi et al., 2022) in a GALLENKAMP® incubator model at 37 °C and 75% humidity. During this period, all eggs were candled daily for viability. Deaths in the first 24 h were assumed to be injection errors or probable bacterial infections and were eliminated from the results. On the 4th day of incubation, each group's live or dead embryos were sorted and evaluated for gross anomalies. Next, the chick embryos were fixed with 10% neutral-buffered formalin for one week. Finally, 4 μm tissue sections were obtained from the whole chick body, including head, thorax, and abdomen, embedded in paraffin and stained with hematoxylin and eosin (H&E) for microscopic studies.

Cytotoxicity assay

Ninety-six-well culture plates with MDCK cells were incubated at 37 °C in a 5% CO_2 atmosphere for one day. Cells were then treated with various concentrations of the peptide, virus, and peptide-treated virus for 24 h with the

Khodayari., et al. (2025). Inhibitory Effect of cLF-chimera on H9N2 Influenza Virus. *Iran J Vet Med, 19*(2):237-254..

239

same condition as the previous step (Table 2 presents all 14 groups in detail). A cell viability assay was performed using the 3-(4,5-dimethylthiazol-2-yl)-2,5 diphenyl tetrazolium bromide) (MTT) method to determine the cytotoxicity of all treatment groups. Briefly, 10 µL of MTT solution was added to each well and incubated for four hours at 37 °C. Next, 50 µL of dimethyl sulfoxide (DMSO) solution (Thermo Fisher Scientific Corporation, USA) was added to the wells. Finally, the solution's optical density was measured at 570 nm using an enzyme-linked immunosorbent assay (ELISA) reader (anthos 2020®) (Bahuguna et al., 2017; Mehrbod et al., 2018).

Computational modeling

The SWISS-MODEL web server modeled the HA, NA, and M2 projections (Waterhouse et al., 2018). The PEP-FOLD web server also modeled the peptide (Shen et al., 2014). Docking complexes prepared with the ClusPro web server (Porter et al., 2017) were opened using PyMOL software (Schrödinger L, 2020). Photos were taken at the ligand-receptor interaction site.

Statistical analysis

Statistical analysis was performed using Graph Pad Prism software, version 8.0 (GraphPad Software, Boston, Massachusetts USA). Data are represented as Mean±SD for each sample. Two-way analysis of variance was used to compare the means.

Results

Injection of peptide and titrated virus to embryonated eggs

After four days of incubation, eggs were candled to identify the viability of the embryos. The results showed 100% vitality at all peptide concentrations (CP1, CP2, and CP3). There was also nearly 100% viability in all V1 (V1P1, V1P2, and V1P3) and V2 (V2P1, V2P2, and V2P3) groups (except a death related to injection error in the V2P2 group). All embryos in V3P1 and V3P2 died, but V3P3 had very high viability (except for two deaths related to injection error in V3P3). All embryos died in

Table 1. All groups of embryonated egg injection

Groups	Treatment
C	No treatment for egg control
CS	Normal saline injection for injection shock control
CV1	10^2 EID50 unit of the virus injection for virus control
CV2	10^4 EID50 unit of the virus injection for virus control
CV3	10^6 EID50 unit of the virus injection for virus control
CP1	Control for 40 µg of the peptide
CP2	Control for 80 µg of the peptide
CP3	Control for 160 µg of the peptide
V1P1	10^2 EID50 unit of the virus + 40 µg of the peptide
V1P2	10^2 EID50 unit of the virus + 80 µg of the peptide
V1P3	10^2 EID50 unit of the virus + 160 µg of the peptide
V2P1	10^4 EID50 unit of the virus + 40 µg of the peptide
V2P2	10^4 EID50 unit of the virus + 80 µg of the peptide
V2P3	10^4 EID50 unit of the virus + 160 µg of the peptide
V3P1	10^6 EID50 unit of the virus + 40 µg of the peptide
V3P2	10^6 EID50 unit of the virus + 80 µg of the peptide
V3P3	10^6 EID50 unit of the virus + 160 µg of the peptide

Abbreviations: EID50: Embryo infective dose 50; C: Control; V: Virus; P: Peptide.

Table 2. All groups of cell culture system

Groups	Treatment
C	No treatment for cell control
CV	Control of the virus (106 EID50)
CP1	Control for 40 μg of the peptide
CP2	Control for 80 μg of the peptide
CP3	Control for 160 μg of the peptide
V1P1	102 EID50 unit of the virus + 40 μg of the peptide
V1P2	102 EID50 unit of the virus + 80 μg of the peptide
V1P3	102 EID50 unit of the virus + 160 μg of the peptide
V2P1	104 EID50 unit of the virus + 40 μg of the peptide
V2P2	104 EID50 unit of the virus + 80 μg of the peptide
V2P3	104 EID50 unit of the virus + 160 μg of the peptide
V3P1	106 EID50 unit of the virus + 40 μg of the peptide
V3P2	106 EID50 unit of the virus + 80 μg of the peptide
V3P1	106 EID50 unit of the virus + 160 μg of the peptide

Abbreviations: EID50: Embryo infective dose 50; C: Control; V: Virus; P: Peptide.

the virus control groups (CV1, CV2, and CV3), as expected. Table 3 presents the results in detail.

Macroscopic and histopathologic lesions observed in embryos

After four days of incubation and determination of the number of live and dead embryos, they were checked for visible gross lesions. Based on these findings, the embryos in the virus controls (CV1, CV2, CV3), V3P1, and V3P2 were dwarf, featherless, and had visible hemorrhagic lesions in some cases. In contrast, the embryos in the remaining groups were larger, feathered, and had no visible lesions (V1, V2, and V3P3). Figure 2 shows prominent macroscopic findings in some groups.

After checking for gross lesions, all embryos were processed and stained with hematoxylin and eosin (H&E) for microscopic studies. The results showed lesions in different organs in the virus control groups (CV1, CV2, and CV3), V3P1, and V3P2. The lesions were more severe in the virus control groups, while no significant histopathological lesions were observed in the other groups. Table 4 and Figure 3 show the histopathological findings in detail.

Histopathological evaluation demonstrated that the target organs were significantly significantly in CV1, CV2, CV3, V3P1, and V3P2 (Table 4):

The major histopathological findings in the brains of the control group included large vacuolation of the neuropil (spongiosis), which was established by edema. Moreover, the blood vessels were congested, and ischemic neuronal changes were scattered throughout the parenchyma.

Massive hemorrhage and congestion in the large and small blood vessels appeared in the renal and perirenal adipose tissues. Intensive tubular necrosis with deep eosinophilic staining was an outstanding finding. Glomeruli were relatively spared from influential damage and the interstitium was invaded by a large population of inflammatory cells, mainly mononuclear cells. Intensive hemorrhage with focal to diffuse hepatocellular degeneration or necrosis with marked congestion of the central veins, small-sized blood vessels, and sinusoids were obvious in the liver. Large pulmonary vascular congestion with hemorrhage in the interstitium was accompanied by large numbers of inflammatory cells in the pulmonary parenchyma. Furthermore, primitive parabronchi had highly exfoliated epithelial cells in their lumen.

Khodayari., et al. (2025). Inhibitory Effect of cLF-chimera on H9N2 Influenza Virus. *Iran J Vet Med*, *19*(2):237-254..

241

Table 3. Number of live and dead embryos in each group

Groups	No.		%
	Live Embryos	Dead Embryos	Livability
C	10	0	100
CS	10	0	100
CV1	0	10	0
CV2	0	10	0
CV3	0	10	0
CP1	10	0	100
CP2	10	0	100
CP3	10	0	100
V1P1	10	0	100
V1P2	10	0	100
V1P3	10	0	100
V2P1	10	0	100
V2P2	9	1	90
V2P3	10	0	100
V3P1	0	10	0
V3P2	0	10	0
V3P3	8	2	80

Abbreviations: C: Control; V: Virus; P: Peptide.

In the eyeball, continuous hemorrhage along the choroid layers with extensive edema was striking. Moreover, severe disruption of the retinal pigmented epithelium or even compete detachment in some embryosit was not identified in the microscopic evaluation. Eventually, hemorrhage and congestion were observed in dermal and hypodermal layers, with degraded collagen fibers in the integument. Other organs with minimal changes were the spleen and intestine, in which the red pulp was filled with erythrocytes, and necrotic villi were detected in only some intestinal tissues.

No noticeable changes were observed in other organs, such as the gizzard, proventriculus, or musculoskeletal system. All organs had a normal architecture similar to the negative control group in the peptide and peptide-virus treatment groups. However, mild to moderate congestion was observed in the V1P1-3, V2P1-3, and V3P3 groups, and scant infiltration of inflammatory cells was present around the central veins with mild hyperplasia of the bile ducts in the liver.

Cytotoxicity assay

We tested different peptide and virus concentrations and studied the mixtures at 570 nm wavelength. The results (Figure 4) showed that the peptide concentration increased in V1 (V1P1, V1P2, and V1P3) and V2 (V2P1, V2P2, and V2P3) groups leading to a decrease in cell viability. All cell viability percentages in the V1 group were lower than those in the V2. In the V3 groups (V3P1, V3P2, and V3P3), unlike V1 and V2, the increase in peptide concentration caused an increase in cell viability.

In the peptide controls (CP1, CP2, and CP3), cell viability decreased with an increase in the amount of peptide. Cell viability was lowest in the virus control group (Figure 4).

Table 4. Histopathological lesions of the groups

Tissue/ Group	C	CS	CV1	CV2	CV3	CP1	CP2	CP3	V1P1	V1P2	V1P3	V2P1	V2P2	V2P3	V3P1	V3P2	V3P3
CNS	0	0	3	3	3	0	0	0	1	1	0	1	1	0	3	2	0
Eyeball	1	0	3	3	3	1	0	1	2	1	1	1	1	0	3	2	0
Lung	0	0	3	3	3	0	0	0	1	0	0	1	0	0	3	3	0
Liver	0	0	3	3	3	0	0	0	0	0	0	0	0	0	3	3	0
Kidney	0	0	3	3	3	0	0	0	0	0	0	0	0	0	3	3	0
Skin	0	0	3	3	3	0	0	0	1	0	0	0	1	0	3	2	1
Proven-triculus	0	0	0	1	1	0	0	0	0	0	0	0	0	0	0	0	0
Intestine	0	1	0	1	1	0	0	0	0	0	0	0	0	0	3	2	0
Spleen	0	0	3	3	3	0	0	0	1	1	1	0	0	0	3	2	1

Abbreviations: C: Control; V: Virus; P: Peptide; CNS: Central nervous system.

Note: Virus: 3 to 1 maximum to minimum concentration; (3: High concentration: 2: Medium concentration: 1: Low concentration); Control; Peptide: 3 to 1 maximum to minimum concentration (3: High concentration: 2: Medium concentration: 1: Low concentration); Pathological observation: (3: Intensive: 2: Moderate: 1: Mild: 0: None).

Computational modeling

We used the SWISS-MODEL and PEP-FOLD web servers to estimate the viral projections and peptide shapes. Then we used the ClusPro web server to evaluate the docking complexes. Figure 5 (A&B) shows the docking complexes and putative interactions between the receptor and ligand amino acids. Molecular docking showed 5, 7, and 13 possible interactions between the peptide and viral M2 ion channel, HA, and NA glycoproteins.

Discussion

The H9N2 subtype of AIV can cause direct and indirect losses in the poultry industry and can be transferred to humans, which is a public health issue (Mostafa et al., 2018; Ali et al., 2019; Perez DR et al., 2019; Swayne et al., 2020). Due to the highly mutative nature of the virus, resistance to current chemical drugs is a common finding (Jones et al., 2006). Since chemical drugs have several side effects (Anand et al., 2019), there is an immediate need for a new group of anti-influenza drugs with less
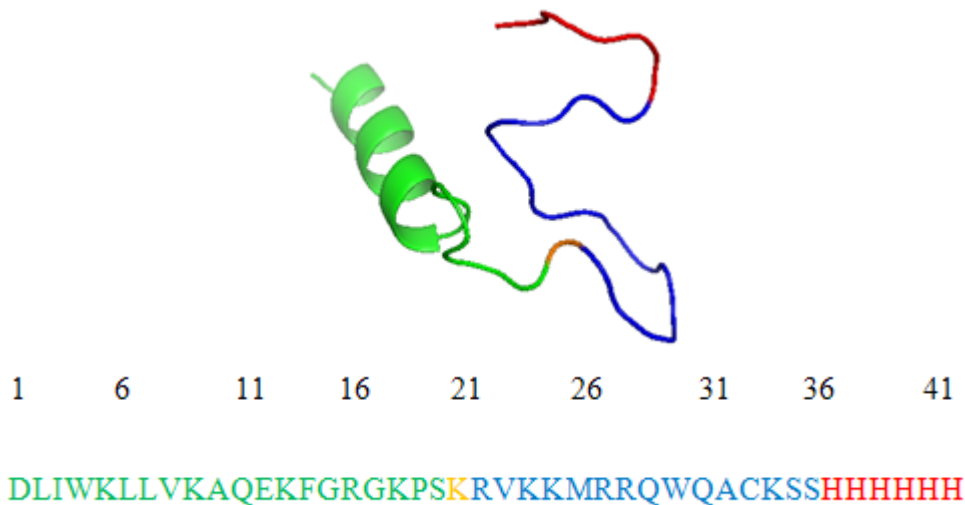
Figure 1. A) The cartoon structure of cLFchimera (Green: cLFampin, Orange: Lysine, Blue: cLFcin, Red: Histidine tag)

B) The sequence of the peptide

Khodayari., et al. (2025). Inhibitory Effect of cLF-chimera on H9N2 Influenza Virus. *Iran J Vet Med, 19*(2):237-254..

243
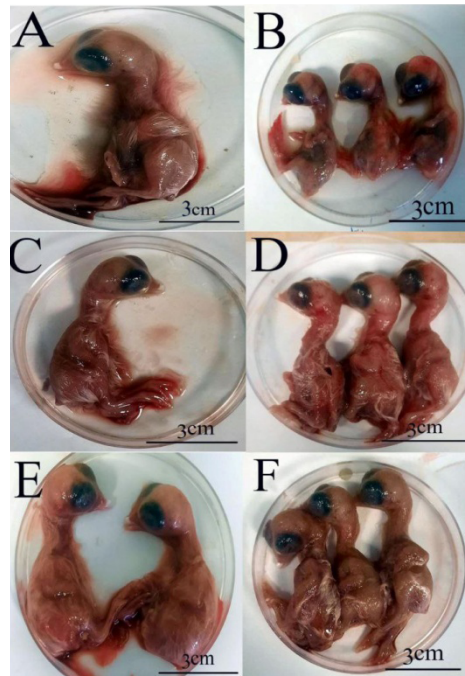
Figure 2. Prominent macroscopic findings of the embryos (A: C, B: CV3, C: CP3, D: V1P1, E: V2P1, F: V3P3)

viral resistance and side effects (Sala et al., 2019). For this purpose, many studies have focused on different drug candidates; one group includes AMPs with anti-influenza properties with broad-spectrum activity (Kang et al., 2017). This study evaluated the anti-influenza effects of a novel chimeric peptide, cLF-chimera, on the H9N2 subtype in embryonated eggs and MDCK cells.

The in ovo model is a standard method evaluating the probable anti-influenza activities of different drug candidates. It is ethical compared to laboratory animal models and is on the edge of in vitro and in vivo models (Ghoke et al., 2018). This study's data from embryonated egg injections (Table 3) showed that the embryos were highly livable without distinct macroscopic lesions (Figure 2) in the peptide control groups. This result is comparable to Michálek et al.'s results that used melittin as an AMP at a concentration of 2 μM, which did not severely affect embryo vitality, and the embryos did not have macroscopic lesions (Michálek et al., 2015). In addition, the histopathological findings in peptide control groups were similar to those of negative control and saline control, without any significant changes (Table 4 and Figure 3). Based on the above data, it can be inferred that the peptide was not toxic to the embryos at the given doses.

In the virus control groups, embryo mortality was 100% (Table 3). The embryos were dwarf and featherless, with visible hemorrhagic lesions in some cases (Figure 2). AIVs cause pathological changes in chicken embryos via apoptosis and necrosis (Ahmadi et al., 2018), and histopathological findings contribute to viral damage. In our study, histopathological results in virus control groups revealed that (Table 4 and Figure 3), except for the gastrointestinal tract with minimal lesions, the other main infected organs were prominently affected and severely damaged. This result is comparable to Shah et al.'s, who evaluated the potential effect of three herbal extracts on the H9N2 subtype in embryos. In their study, positive controls were severely damaged in different organs (Liver, spleen, bursa) (Shah et al., 2021). The virus is harmful to embryos at the given doses.

Our results revealed that the embryos were livable in all V1 and V2 groups (Table 3), without distinct macroscopic lesions (Figure 2). The histopathological findings in all these groups showed mild lesions in some cases (Table 4 and Figure 3). According to the results, the peptide in all V1 and V2 groups at given doses could prevent the adverse effects of different virus concentrations in ovo. These data (especially embryo survival rate) are comparable with those of the study by Sauerbrei et al. on the H9N2 subtype (Sauerbrei et al., 2006). In this study, four anti-influenza drugs were evaluated against 102 and 1 EID50 units of the virus: Amantadine, rimantadine, oseltamivir, and zanamivir, with the highest embryo survival rates of 21.9% for adamantanes and 50% for neuraminidase inhibitors (Sauerbrei et al., 2006).

In the V3P1 and V3P2 groups, the embryo survival rate is zero (Table 3), and embryos are dwarf and featherless, with apparent macroscopic lesions (such as hemorrhagic lesions) in some cases (Figure 2). Histopathologically, severe lesions were detected in these groups (similar to virus controls, but the lesions were less severe, and the V3P2 group had less severe lesions than the V3P1) (Table 4 and Figure 3). These data also indicated that low and medium peptide concentrations could not entirely prevent destructive viral effects in embryos. In the V3P3 group, the survival rate is very high (except for deaths due to injection errors) (Table 3), and the embryos have no noticeable macroscopic lesions (Figure 2). From a histopathological point of view, the findings are similar to those of the peptide control, negative control, saline

control, and all V1 and V2 groups (Table 4) without any significant changes (Figure 3). Based on the data obtained from the V3 group, it is deduced that the peptide could prevent the adverse effects of the virus in a dose-dependent manner.

The MTT assay is a color-based assay that evaluates the metabolic activity of cells. The assay is routine, easy, and advantageous for animal cell lines (Tolosa et al., 2015). According to the results obtained from the MTT assay in the peptide control groups (Figure 4), cell viability decreased as the peptide dose increased. This result suggested that the peptide is toxic to the cell line in a dose-dependent manner. These data are consistent with previous studies on different antiviral peptides in differ-

A)

B)

C)

D)

Khodayari., et al. (2025). Inhibitory Effect of cLF-chimera on H9N2 Influenza Virus. *Iran J Vet Med, 19*(2):237-254..

245

E)

F)
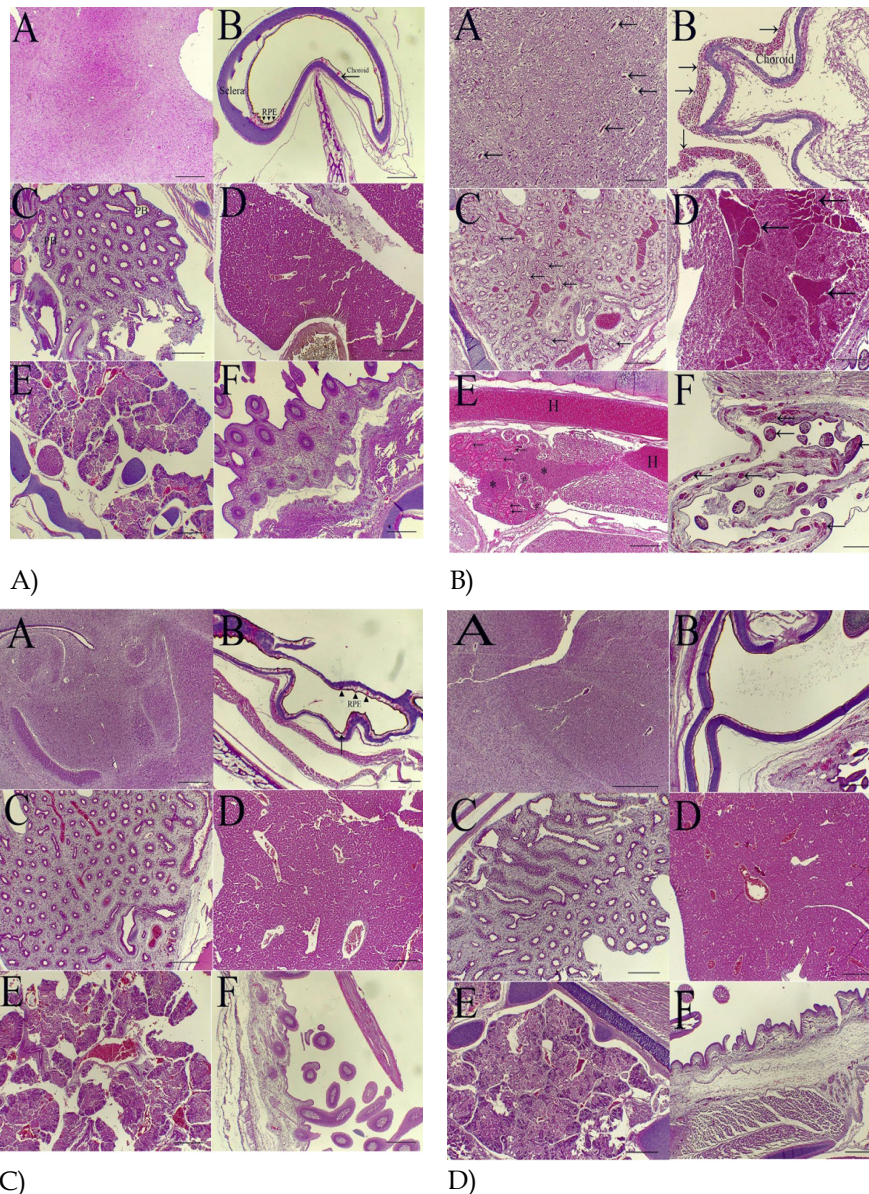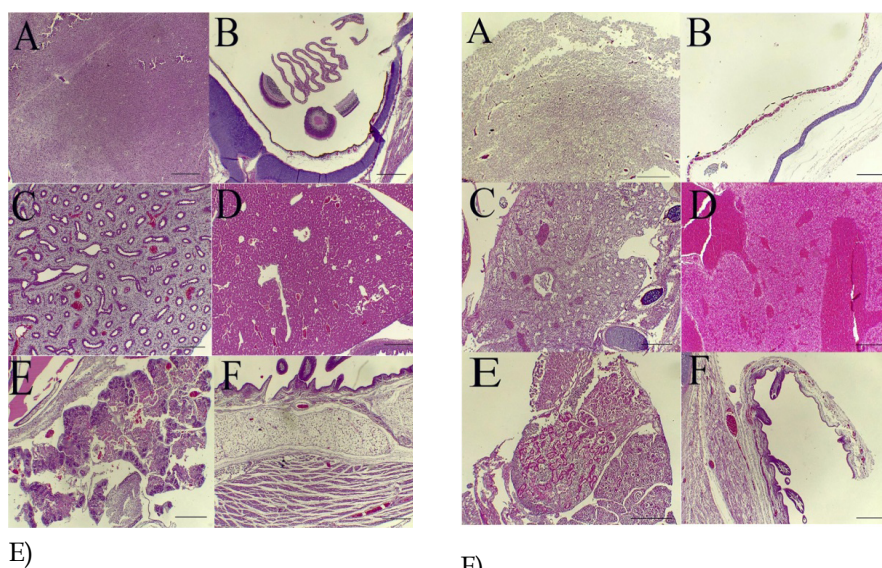
Figure 3. Histopathological lesions in some groups

A) C & CS groups, normal structures of chicken embryo

Note: Brain: Neuropil is intact (a). Eyeball: A few thin-walled vessels are congested in the choroid layer. RPE (retinal pigmented epithelium) is continuously preserved. (b). Lung: primitive parabronchi (PB) with cuboidal epithelium embedded in slightly alveolar (loose fibrous) connective tissue (c). Liver: large blood vessels and sinusoids are clear and only a few vessels are congested in a lesser extent (d). Kidney: The glomeruli, and tubules were normal, and some blood vessels were congested (e). Skin: normal architecture of feather follicles and epidermal-dermal structure (f). HE. Scale bar (a-f) 400 μm.

B) Virus control groups (CV1, CV2, CV3)

Note: Brain: Status spongiosis of the neuropil (vacoulation). The blood vessels are intensively congested. The prevascular spaces are significantly extended by edema (arrows) (a). Eyeball: The retinal pigmented epithelial layer (RPE) is completely detached, and the choroid is extensively congested and hemorrhagic (arrows) (b). Lung: intensive vascular congestion of the vessels and accumulation of red blood cells and inflammatory cells in the parenchyma. The epithelial cells of parabronchi are largely desquamated into the lumen (arrows) (c). Liver: Massive congestion of central veins and hemorrhage in the parenchyma (arrows). The spaces of Disse are impacted with erythrocytes and focal areas of hepatocellular degeneration or necrosis are evident (d). Kidney: Renal disruption with intensive hemorrhage in the parenchyma and perirenal tissue (H) along with necrosis of tubular epithelial cells that are markedly hyalinized (arrows). A large focal population of inflammatory cells was present (asterisks). Scant degeneration of glomeruli (g) is observed (e). Skin: Widespread bleeding and congestion of the vessels in the dermis with prominent mononuclear cell infiltration (f). HE. Scale bar: 150 μm and (b-f) 400 μm.

C) Protein control groups (CP1, CP2, CP3)

Note: Brain; normal architecture of neuropil (a). Eyeball: A few microvessels are in the choroid layer engorged with erythrocytes (arrow). The retinal pigmented epithelial layer (RPE) is intact (arrowheads) (b). Lung: Parabronchi are normal, and some vessels are markedly congested (c). Liver: The structure is normal. A few central veins are dilated (d). Kidney: Normal renal structure with large, thin-walled, congested blood vessels (e). Skin: Normal anatomy of epidermal-dermal layer (f). HE. Scale bar (A-F) 400 μm.

D)Virus protein groups (V1P1, V1P2, V1P3), intact and normal structures of all histological specimens

Note: Brain (a), Eyeball (b), Lung (c), Liver (d), Kidney (e), and Skin (f). HE. Scale bar (a-f) 400 μm.

E) Virus protein groups (V2P1, V2P2, V2P3), all tissue structures in normal position

Note: Brain (a), eyeball (b), lung (c), liver (d), kidney (e), and skin (f). HE. Scale bar (a-f) 400 μm.

F) Virus protein groups (V3P1 & V3P2)

Note: Brain: Status spongiosis of neuropil. Marked small and medium-sized blood vessel congestion with relatively large perivascular edematous spaces (a). Eyeball: The choroid is extremely wide with a large amount of edema. In the outermost choroid layer, a chain structure of microvessels is highly congested, and the retinal pigmented epithelium is strongly disrupted (b). Lung: The disorganized architecture of pulmonary parenchyma. The parabronchial epithelial lining is necrotic and exfoliated into the lumen. The interstitial tissue is invaded by inflammatory and red blood cells, and most of the air capillaries and vessels are congested (c). Liver: Extensive hemorrhage in parenchyma and severe congestion from Disse spaces to large blood vessels. Also, a smaller population of inflammatory cells among the erythrocytes are dispersed in the parenchyma (d). Kidney: Massive necrosis of tubular cells, designated as intense eosinophilic structures (e). Skin: Tiny to large blood vessels are highly impacted by red blood cells and hemorrhage admixed with inflammatory cells, principally at the dermal-epidermal junction. Collagen fibers are degenerated in the deep dermal layer (f). HE. Scale bar (A-F) 400 μm.

G) Virus protein group (V3P3) normal histological architecture of all organs is demonstrated

Note: Only mild to moderate congestion in the liver (d), kidney (e), skin (f), brain (a), eyeball (b), and lung (c), HE, scale bar (A-F) 400 μm.
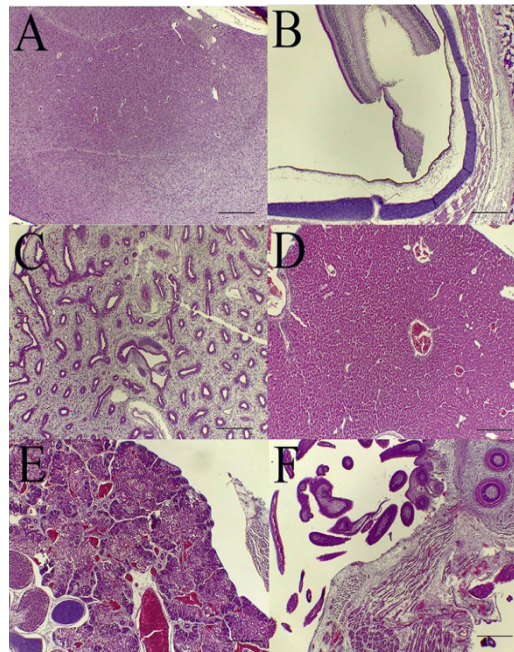
Figure 4. Cell viability in different groups correlated to peptide and virus concentrations

*P<0.05; ****P<0.00001, Ns: P>0.05.

ent cell lines (Sala et al., 2019; De Angelis et al., 2021). Overall, our results indicated that the peptide was toxic to the cell line, but not to the embryo. This difference can result from a lack of defense mechanisms and higher sensitivity of cells in the cell culture system compared to the body (Hartung, 2007).

We also discovered that the virus control group had the lowest percentage of cell viability (Table 5). The low percentage may be due to the virus's cytopathic effects (CPE) (Chen et al., 2022). These data show that both the peptide and the virus harmed cell viability, but the virus's effect is much higher.

Our study showed that in the V1 groups, cell viability decreased as the peptide dose increased, and V1P1 had the best cell viability (Figure 4). The cell viability percentage of these groups is lower than the same dose of peptide controls. However, it is higher than virus control (except V1P3, which is higher than P3 alone, but with a minimum difference) (Figure 4). The peptide in the V1P3 group can block the viral effect, and the remaining peptide has lower toxicity than P3 alone. As the viral dose is constant in these groups, it is more probable that the decrease in cell viability is related to peptide toxicity. Simultaneously, the peptide can partially prevent the destructive effects of the virus.

The data from V2 groups are similar to those of V1, but all cell viability percentages are higher (Figure 4). In these groups, like V1, the amount of virus is constant; the decrease in cell vitality is related to peptide toxicity. Compared to the virus control, in the V2 groups, the peptide partially inhibited the harmful effects of the virus.

In the V3 groups, our data showed that, unlike V1 and V2, the increase in the peptide dose caused an increase in cell viability (Figure 4). All percentages were higher than those of the virus control but lower than those of the peptide controls. Because the virus concentration is constant, the decrease in V3P1 and V3P2 is much higher than in previous groups, and it is close to the virus control; it might primarily result from a viral cytopathogenic effect (CPE). However, the peptide could partially block the virus's adverse effects even in this group.

Based on the data obtained in these three groups, the peptide can be inferred to inhibit destructive viral effects in all groups. Our study also revealed that the optimum peptide dose in the V1, V2, and V3 groups were V1P1, V2P1, and V3P3, respectively.

Molecular docking is a drug design procedure that anticipates the binding form and mimics the molecular interaction between a ligand and receptor (Fan et al., 2019). In our study, we evaluated the interaction between the peptide, viral surface glycoproteins (HA and NA), and M2 ion channels by molecular docking to de-

Khodayari., et al. (2025). Inhibitory Effect of cLF-chimera on H9N2 Influenza Virus. *Iran J Vet Med, 19*(2):237-254..

247
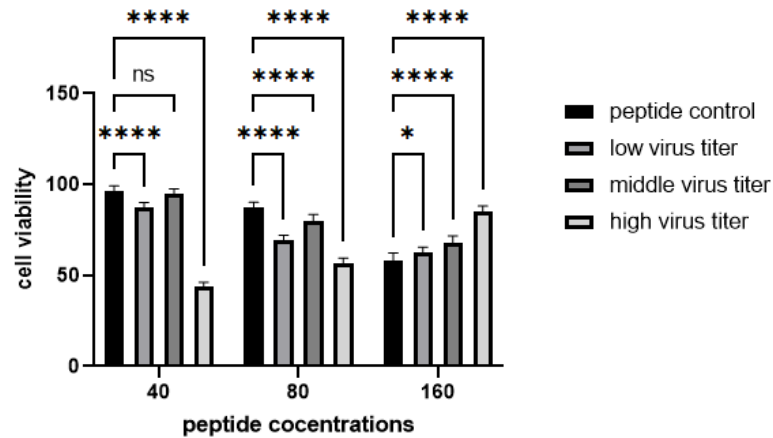
A
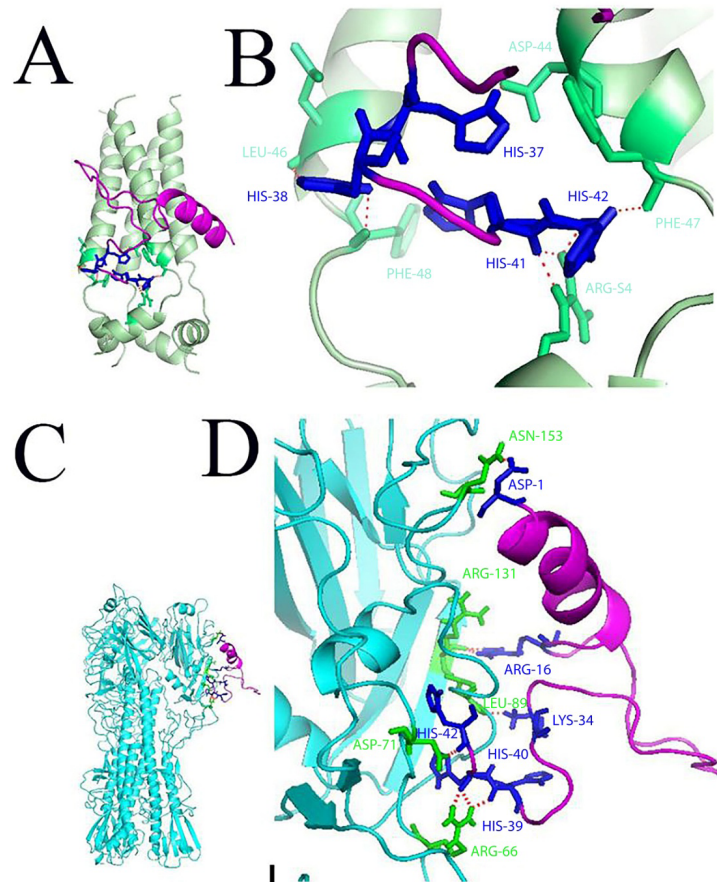
B

Figure 5. A) The results of molecular docking between the peptide, the virus M2 ion channel, and HA glycoprotein

Note: A & B, M2 ion channel; Green, the M2 ion channel; deep green, amino acid residues of M2 at interaction site; violet, the peptide; deep blue, amino acid residues of the peptide at interaction site; C & D, HA glycoprotein; cyan, the HA glycoprotein; green, amino acid residues of HA at interaction site; violet, the peptide; deep blue, amino acid residues of the peptide at inter-action site.

B) The results of molecular docking between the peptide and the virus NA glycoprotein

Note: E & F: Wheat, the NA glycoprotein; deep pink, amino acid residues of NA at interaction site; violet, the peptide; deep blue, amino acid residues of the peptide at interaction site.

termine the probable mechanism of action of the peptide. According to the docking results (Figure 5), the M2 ion channel has five possible interactions with the peptide. According to the previous studies on Adamantane's action mechanism, amino acid residue ASP-44 is a site of action for these drugs (Rosenberg & Casarotto 2010; Özbil, 2019). Thus, the peptide may mimic Adamantane's action mechanism by blocking the M2 ion channel (Figures 5A and 5B).

The docking complex between the peptide and viral HA showed seven potential peptide attachment residues. Based on previous studies on drugs that block the HA glycoprotein, amino acids ASN-153 and ARG-131 are in the receptor-binding site of HA1 (Yang et al., 2013). Therefore, the peptide may prevent the virus from attaching to cellular receptors (Figures 5C and 5D).

Our docking results also showed 13 possible interaction sites between the peptide and viral NA glycoprotein (Figures 5E and 5F). Based on previous studies on NA blockers, none of these interaction sites play a role in blocking NA glycoproteins. However, due to the high number of potential attachment sites, further studies are required, which can be a subject for future studies on cLF-chimeras.

Finally, AMPs, such as cLF-chimeras, can have different potential modes of action. Some action mechanisms include inhibition of virus attachment and cell membrane fusion, disruption of the viral envelope, inhibition of viral replication, and other probable mechanisms (Skalickova et al., 2015). Therefore, the anti-influenza effect of the peptide in this study can be due to a combination of the mechanisms above.

The cLF-chimera has also proven its effects against bacteria participating in respiratory complexes (Tanhaiean et al., 2018a; Tanhaieian et al., 2018b; Roshanak et al., 2020; Tanhaeian & Sekhavati et al., 2020). This study also suggests that this peptide has potential anti-influenza properties. Since the H9N2 subtype can mainly cause respiratory disease in poultry (Nili & Asasi, 2003; Swayne et al., 2020) and flu-like, mild, primarily respiratory illness in human populations (Liu et al., 2018; Song & Qin, 2020), the peptide can affect viruses and other secondary bacteria. Compared to common anti-influenza drugs, this broad-spectrum impact is advantageous for the peptide.

In most viral respiratory diseases, the primary viral agents are accompanied by secondary infections (Seto et al., 2013, Swayne et al., 2020). However, further stud-

ies are needed to explain these peptides' potential pros and cons as drug candidates. This study elucidates some peptide characteristics with some undefined questions regarding its novelty: How to use it in vivo? how can we determine its precise dosage and the exact mechanism of action? These topics are beyond the scope of this study but can be evaluated in future studies.

Ethical Considerations

Compliance with ethical guidelines

This study was approved by the Animal Ethics Committee of the University of Tehran, Tehran, Iran (Code: IR.UT.VETMED.REC.1401.004).

Funding

Authors' contributions

All authors contributed equally to the conception and design of the study, data collection and analysis, interception of the results and drafting of the manuscript. Each author approved the final version of the manuscript for submission.

Conflict of interest

The authors declared no conflict of interest.

References

Ahmadi, S., Rajabi, Z., & Vasfi-Marandi, M. (2018). Evaluation of the antiviral effects of aqueous extracts of red and yellow onions (Allium Cepa) against avian influenza virus subtype H9N2. *Iranian Journal of Veterinary Science and Technology, 10*(2), 23-27. [DOI:10.22067/veterinary.v2i10.74060]

Abdi, H. M., Mayahi, M., Boroomand, Z., & Shoshtari, A. (2021). Avian Influenza-Killed Vaccine on Tissue Distribution and Shedding of Avian Influenza Virus H9N2 in Ducklings. *Archives of Razi Institute, 76*(3), 437–444. [DOI:10.22092/ari.2020.342078.1452]

Ali, M., Yaqub, T., Mukhtar, N., Imran, M., Ghafoor, A., & Shahid, M. F., et al. (2019). Avian influenza A (H9N2) virus in poultry worker, Pakistan, 2015. *Emerging Infectious Diseases, 25*(1), 136–139. [DOI:10.3201/eid2501.180618] [PMID]

Khodayari., et al. (2025). Inhibitory Effect of cLF-chimera on H9N2 Influenza Virus. *Iran J Vet Med, 19*(2):237-254..

249

Amarelle, L., Lecuona, E., & Sznajder, J. I. (2017). Anti-influenza treatment: Drugs currently used and under development. *Tratamiento Antigripal: Fármacos Actualmente Utilizados y Nuevos Agentes en Desarrollo. Archivos de Bronconeumologia, 53*(1), 19–26. [DOI:10.1016/j.arbres.2016.07.004] [PMID]

Anand, U., Jacobo-Herrera, N., Altemimi, A., & Lakhssassi, N. (2019). A comprehensive review on medicinal plants as antimicrobial therapeutics: Potential avenues of biocompatible drug discovery. *Metabolites, 9*(11), 258. [DOI:10.3390/metabo9110258] [PMID]

Arbi, M., Larbi, I., Nsiri, J., Behi, I. E., Rejeb, A., & Miled, K., et al. (2022). Inhibition of avian influenza virus H9N2 infection by antiviral hexapeptides that target viral attachment to epithelial cells. *Virus Research, 313,* 198745. [DOI:10.1016/j.virusres.2022.198745] [PMID]

Bahar, A. A., & Ren, D. (2013). Antimicrobial peptides. *Pharmaceuticals, 6*(12), 1543-1575. [DOI:10.3390/ph6121543] [PMID]

Bahuguna, A., Khan, I., Bajpai, V. K., & Kang, S. C. (2017). MTT assay to evaluate the cytotoxic potential of a drug. *Bangladesh Journal of Pharmacology, 12*(2), 115-118. [Link]

Chen, H., Yuan, H., Gao, R., Zhang, J., Wang, D., & Xiong, Y., et al. (2014). Clinical and epidemiological characteristics of a fatal case of avian influenza A H10N8 virus infection: A descriptive study. *Lancet (London, England), 383*(9918), 714–721. [DOI:10.1016/S0140-6736(14)60111-2] [PMID]

Chen, J. J., Lin, P. H., Lin, Y. Y., Pu, K. Y., Wang, C. F., & Lin, S. Y., et al. (2022). Detection of cytopathic effects induced by influenza, parainfluenza, and enterovirus using deep convolution neural network. *Biomedicines, 10*(1), 70. [DOI:10.3390/biomedicines10010070] [PMID]

Daneshmand, A., Kermanshahi, H., Sekhavati, M. H., Javadmanesh, A., & Ahmadian, M. (2019). Antimicrobial peptide, cLF36, affects performance and intestinal morphology, microflora, junctional proteins, and immune cells in broilers challenged with E. coli. *Scientific Reports, 9*(1), 14176. [DOI:10.1038/s41598-019-50511-7] [PMID]

Daneshmand, A., Kermanshahi, H., Sekhavati, M. H., Javadmanesh, A., Ahmadian, M., & Alizadeh, M., et al. (2020). Effects of cLFchimera peptide on intestinal morphology, integrity, microbiota, and immune cells in broiler chickens challenged with necrotic enteritis. *Scientific Reports, 10*(1), 17704. [DOI:10.1038/s41598-020-74754-x] [PMID]

De Angelis, M., Casciaro, B., Genovese, A., Brancaccio, D., Marcocci, M. E., & Novellino, E., et al. (2021). Temporin G, an amphibian antimicrobial peptide against influenza and parainfluenza respiratory viruses: Insights into biological activity and mechanism of action. *FASEB Journal: Official Publication of the Federation of American Societies for Experimental Biology, 35*(2), e21358. [DOI:10.1096/fj.202001885RR] [PMID]

Fan, J., Fu, A., & Zhang, L. (2019). Progress in molecular docking. *Quantitative Biology, 7,* 83-89. [Link]

Ghoke, S. S., Sood, R., Kumar, N., Pateriya, A. K., Bhatia, S., & Mishra, A., et al. (2018). Evaluation of antiviral activity of Ocimum sanctum and Acacia arabica leaves extracts against H9N2 virus using embryonated chicken egg model. *BMC Complementary and Alternative Medicine, 18*(1), 174. [DOI:10.1186/s12906-018-2238-1] [PMID]

Hartung, T. (2007) Food for thought... on cell culture. *ALTEX, 24*(3), 143–152. [DOI:10.14573/altex.2007.3.143]

Hussain, M., Galvin, H. D., Haw, T. Y., Nutsford, A. N., & Husain, M. (2017). Drug resistance in influenza A virus: The epidemiology and management. *Infection and Drug Resistance, 10,* 121–134. [DOI:10.2147/IDR.S105473] [PMID]

Jones, J. C., Turpin, E. A., Bultmann, H., Brandt, C. R., & Schultz-Cherry, S. (2006). Inhibition of influenza virus infection by a novel antiviral peptide that targets viral attachment to cells. *Journal of Virology, 80*(24), 11960–11967. [DOI:10.1128/JVI.01678-06] [PMID]

Kang, H. K., Kim, C., Seo, C. H., & Park, Y. (2017). The therapeutic applications of antimicrobial peptides (AMPs): A patent review. *Journal of Microbiology (Seoul, Korea), 55*(1), 1–12. [DOI:10.1007/s12275-017-6452-1] [PMID]

Koszalka, P., Tilmanis, D., & Hurt, A. C. (2017). Influenza antivirals currently in late-phase clinical trial. *Influenza and Other Respiratory Viruses, 1*1(3), 240–246. [DOI:10.1111/irv.12446] [PMID]

Lam, T. T., Wang, J., Shen, Y., Zhou, B., Duan, L., & Cheung, C. L., et al. (2013). The genesis and source of the H7N9 influenza viruses causing human infections in China. *Nature, 502*(7470), 241–244. [DOI:10.1038/nature12515] [PMID]

Lehnert, R., Pletz, M., Reuss, A., & Schaberg, T. (2016). Antiviral medications in seasonal and pandemic influenza: A systematic review. *Deutsches Arzteblatt International, 113*(47), 799–807. [DOI:10.3238/arztebl.2016.0799] [PMID]

Lei, J., Sun, L., Huang, S., Zhu, C., Li, P., & He, J., et al. (2019). The antimicrobial peptides and their potential clinical applications. *American Journal of Translational Research, 11*(7), 3919-3931. [PMID]

Li, Q., Zhao, Z., Zhou, D., Chen, Y., Hong, W., & Cao, L., et al. (2011). Virucidal activity of a scorpion venom peptide variant mucroporin-M1 against measles, SARS-CoV and influenza H5N1 viruses. *Peptides, 32*(7), 1518–1525. [DOI:10.1016/j.peptides.2011.05.015] [PMID]

Liu, R., Zhao, B., Li, Y., Zhang, X., Chen, S., & Chen, T. (2018). Clinical and epidemiological characteristics of a young child infected with avian influenza A (H9N2) virus in China. *The Journal of International Medical Research, 46*(8), 3462–3467. [DOI:10.1177/0300060518779959] [PMID]

Mehrabadi, M. H. F., Ghalyanchilangeroudi, A., Rabiee, M. H., & Tehrani, F. (2019). Prevalence and risk factors of avian influenza H9N2 among backyard birds in Iran in 2015. *Asian Pacific Journal of Tropical Medicine, 12*(12), 559-564. [Link]

Mehrbod, P., Abdalla, M. A., Njoya, E. M., Ahmed, A. S., Fotouhi, F., & Farahmand, B., et al. (2018). South African medicinal plant extracts active against influenza A virus. *BMC Complementary and Alternative Medicine, 18*(1), 112. [DOI:10.1186/s12906-018-2184-y] [PMID]

Meng, X. Y., Zhang, H. X., Mezei, M., & Cui, M. (2011). Molecular docking: a powerful approach for structure-based drug discovery. *Current Computer-Aided Drug Design, 7*(2), 146–157. [DOI:10.2174/157340911795677602] [PMID]

Michálek, P., O. Zítka, R. Guráň, V. Milosavljevič, P. Kopel, V. Adam and Z. Hegar (2015). Effect of melittin on influenza-infected chicken embryos, MendelNet. 2015, 475-479. [Link]

250

Khodayari., et al. (2025). Inhibitory Effect of cLF-chimera on H9N2 Influenza Virus. *Iran J Vet Med, 19*(2):237-254..

Mohammadi, E., Sekhavati, M. H., Pirkhezranian, Z., Shafizade, N., Dashti, S., & Saedi, N. (2023). Designing and computational analysis of chimeric avian influenza antigen: A yeast-displayed universal and cross-protective vaccine candidate. *Journal of Poultry Sciences and Avian Diseases, 1*(1). [DOI:10.61838/kman.jpsad.1.1.1]

Mostafa, A., Abdelwhab, E. M., Mettenleiter, T. C., & Pleschka, S. (2018). Zoonotic potential of influenza A viruses: A comprehensive overview. *Viruses, 10*(9), 497. [DOI:10.3390/v10090497] [PMID]

Motamedinasab, S. I., Pourbakhsh, S. A., & Nazarpak, H. H. (2023). Evaluation of inactivated vaccine's Antibody response to different H9N2 Vaccination programs with Hemagglutination Inhibition (HI) assay. *Journal of Poultry Sciences and Avian Diseases, 1*(3), 51-58. [DOI:10.61838/kman.jpsad.1.3.5]

Nagy, A., Mettenleiter, T. C., & Abdelwhab, E. M. (2017). A brief summary of the epidemiology and genetic relatedness of avian influenza H9N2 virus in birds and mammals in the Middle East and North Africa. *Epidemiology and Infection, 145*(16), 3320–3333. [DOI:10.1017/S0950268817002576] [PMID]

Nili, H., & Asasi, K. (2003). Avian influenza (H9N2) outbreak in Iran. *Avian Diseases, 47*(3 Suppl), 828–831. [DOI: 10.1637/0005-2086-47.s3.828] [PMID]

Ong, Z. Y., Wiradharma, N., & Yang, Y. Y. (2014). Strategies employed in the design and optimization of synthetic antimicrobial peptide amphiphiles with enhanced therapeutic potentials. *Advanced Drug Delivery Reviews, 78,* 28–45. [DOI:10.1016/j.addr.2014.10.013] [PMID]

Özbil, M. (2019). Computational investigation of influenza A virus M2 protein inhibition mechanism by ion channel blockers. *Turkish Journal of Chemistry, 43*(1), 335-351. [Link]

Pagadala, N. S., Syed, K., & Tuszynski, J. (2017). Software for molecular docking: A review. *Biophysical Reviews, 9*(2), 91–102. [DOI:10.1007/s12551-016-0247-1] [PMID]

Peacock, T. H. P., James, J., Sealy, J. E., & Iqbal, M. (2019). A global perspective on H9N2 avian influenza virus. *Viruses, 11*(7), 620. [DOI:10.3390/v11070620] [PMID]

Perez DR, C. S., Cardenas-Garcia S, Ferreri LM., Santos J, Rajao DS., Poole. (2019) Avian Influenza Virus. Samal SK (ed), *Avian Virology current research and future trends*. Poole; Caister Academic Press.

Pirkhezranian, Z., Tahmoorespur, M., Daura, X., Monhemi, H., & Sekhavati, M. H. (2020). Interaction of camel Lactoferrin derived peptides with DNA: A molecular dynamics study. *BMC Genomics, 21*(1), 60. [DOI:10.1186/s12864-020-6458-7] [PMID]

Porter, K. A., Xia, B., Beglov, D., Bohnuud, T., Alam, N., & Schueler-Furman, O., et al. (2017). ClusPro PeptiDock: Efficient global docking of peptide recognition motifs using FFT. *Bioinformatics (Oxford, England), 33*(20), 3299–3301. [DOI:10.1093/bioinformatics/btx216] [PMID]

Pusch, E. A., & Suarez, D. L. (2018). The Multifaceted Zoonotic Risk of H9N2 Avian Influenza. *Veterinary Sciences, 5*(4), 82. [DOI:10.3390/vetsci5040082] [PMID]

Radmehri, M., Talebi, A., Mousaviyan, S. M., Gholipour, M. A. J., & Taghizadeh, M. (2021). Comparative study on the efficacy of MF 59, ISA70 VG, and nano-aluminum hydroxide adjuvants, alone and with nano-selenium on humoral immunity induced by a bivalent newcastle+ avian influenza vaccine in chickens. *Archives of Razi Institute, 76*(5), 1213-1220. [PMID]

Rajik, M., Jahanshiri, F., Omar, A. R., Ideris, A., Hassan, S. S., & Yusoff, K. (2009). Identification and characterisation of a novel anti-viral peptide against avian influenza virus H9N2. *Virology Journal, 6,* 74. [DOI:10.1186/1743-422X-6-74] [PMID]

Rosenberg, M. R., & Casarotto, M. G. (2010). Coexistence of two adamantane binding sites in the influenza A M2 ion channel. *Proceedings of the National Academy of Sciences of the United States of America, 107*(31), 13866–13871. [DOI:10.1073/pnas.1002051107] [PMID]

Roshanak, S., Pirkhezranian, Z., Shahidi, F., & Hadi Sekhavati, M. (2020). Antibacterial activity of cLFchimera and its synergistic potential with antibiotics against some foodborne pathogens bacteria. [Link]

Sala, A., Ardizzoni, A., Ciociola, T., Magliani, W., Conti, S., & Blasi, E., et al. (2019). Antiviral activity of synthetic peptides derived from physiological proteins. *Intervirology, 61*(4), 166–173. [DOI:10.1159/000494354] [PMID]

Sauerbrei, A., Haertl, A., Brandstaedt, A., Schmidtke, M., & Wutzler, P. (2006). Utilization of the embryonated egg for in vivo evaluation of the anti-influenza virus activity of neuraminidase inhibitors. *Medical Microbiology and Immunology, 195*(2), 65–71. [DOI: 10.1007/s00430-005-0002-x] [PMID]

Schrödinger L, D. W. (2020) PyMOL. Retrieved from: [Link]

Seto, W., J. Conly, C. Pessoa-Silva, Malik, M., & Eremin, S. (2013). Infection prevention and control measures for acute respiratory infections in healthcare settings: An update. *Eastern Mediterranean Health Journal, 19* (Suppl 1), S39-47. [DOI:10.26719/2013.19.supp1.S39]

Shah, S. I. A., Tipu, M. Y., Aslam, A., Khan, A. U., Shafee, M., & Khan, S. A., et al. (2021). Elucidating antiviral activity of Curcuma longa against H9 N2 influenza virus using embryonated chicken egg model. *Tropical Biomedicine, 38*(3), 353–359. [DOI:10.47665/tb.38.3.078] [PMID]

Sharif, A., & Ahmad, T. (2018). Preventing vaccine failure in poultry flocks. In N. Wang & T. Wang (Eds.), *Immunization - Vaccine Adjuvant Delivery System and Strategies*. London: IntechOpen. [DOI:10.5772/intechopen.79330]

Shen, H., Wu, B., Li, G., Chen, F., Luo, Q., & Chen, Y., et al. (2014). H9N2 subtype avian influenza viruses in China: Current advances and future perspectives. *Hosts and Viruses, 1*(2), 54-63. [Link]

Shen, Y., Maupetit, J., Derreumaux, P., & Tufféry, P. (2014). Improved PEP-FOLD approach for peptide and miniprotein structure prediction. *Journal of Chemical Theory and Computation, 10*(10), 4745–4758. [DOI:10.1021/ct500592m] [PMID]

Marashi, S. M., Sheykhi, N., Modirrousta, H., Nikbakht Broujeni, G., Vasfimarandi, M., & Fereidouni, S. (2021). Surveillance of Highly Pathogenic Avian Influenza Viruses (H5Nx Subtypes) in Wild Birds in Iran, 2014-2019. *Archives of Razi Institute, 76*(3), 487–498. [PMID]

Skalickova, S., Heger, Z., Krejcova, L., Pekarik, V., Bastl, K., & Janda, J., et al. (2015). Perspective of use of antiviral peptides against influenza virus. *Viruses, 7*(10), 5428–5442. [DOI:10.3390/v7102883] [PMID]

Song, W., & Qin, K. (2020). Human-infecting influenza A (H9N2) virus: A forgotten potential pandemic strain? *Zoonoses and Public Health, 67*(3), 203–212. [DOI:10.1111/zph.12685] [PMID]

Khodayari., et al. (2025). Inhibitory Effect of cLF-chimera on H9N2 Influenza Virus. *Iran J Vet Med, 19*(2):237-254..

251

Swayne, D. E., Suarez, D. L., & Sims, L. D. (2020). Influenza. In D. E. Swayne, M. Boulianne, Ch. M. Logue, L. R. McDougald, V. Nair, & D. L Suarez (Eds.), *Diseases of Poultry* (pp. 210-256). New Jersey: John Wiley & Sons, Inc. [DOI:10.1002/9781119371199. ch6]

Tahmoorespur, M., Azghandi, M., Javadmanesh, A., Meshkat, Z., & Sekhavati, M. H. (2020). A novel chimeric anti-HCV peptide derived from camel lactoferrin and molecular level insight on its interaction with E2. *International Journal of Peptide Research and Therapeutics, 26,* 1593-1605. [DOI:10.1007/s10989-019-09972-7]

Tanhaeian, A., Sekhavati, M. H., & Moghaddam, M. (2020). Antimicrobial activity of some plant essential oils and an antimicrobial-peptide against some clinically isolated pathogens. *Chemical and Biological Technologies in Agriculture, 7,* 1-11. [Link]

Tanhaiean, A., Azghandi, M., Razmyar, J., Mohammadi, E., & Sekhavati, M. H. (2018). Recombinant production of a chimeric antimicrobial peptide in E. coli and assessment of its activity against some avian clinically isolated pathogens. *Microbial Pathogenesis, 122,* 73–78. [DOI:10.1016/j.micpath.2018.06.012] [PMID]

Tanhaieian, A., Sekhavati, M. H., Ahmadi, F. S., & Mamarabadi, M. (2018). Heterologous expression of a broad-spectrum chimeric antimicrobial peptide in Lactococcus lactis: Its safety and molecular modeling evaluation. *Microbial Pathogenesis, 125,* 51–59. [DOI:10.1016/j.micpath.2018.09.016] [PMID]

Tare, D. S., & Pawar, S. D. (2015). Use of embryonated chicken egg as a model to study the susceptibility of avian influenza H9N2 viruses to oseltamivir carboxylate. *Journal of Virological Methods, 224,* 67–72. [DOI:10.1016/j.jviromet.2015.08.009] [PMID]

Tolosa, L., Donato, M. T., & Gómez-Lechón, M. J. (2015). General cytotoxicity assessment by means of the MTT assay. *Methods in Molecular Biology (Clifton, N.J.), 1250,* 333–348. [DOI:10.1007/978-1-4939-2074-7_26] [PMID]

Torres, N. I., Noll, K. S., Xu, S., Li, J., Huang, Q., & Sinko, P. J., et al. (2013) Safety, formulation and in vitro antiviral activity of the antimicrobial peptide subtilosin against herpes simplex virus type 1. *Probiotics and Antimicrobial Proteins, 5*(1), 26–35. [DOI:10.1007/s12602-012-9123-x] [PMID]

Tripathi, A., & Bankaitis, V. A. (2017). Molecular docking: From lock and key to combination lock. *Journal of Molecular Medicine and Clinical Applications, 2*(1), 10.16966/2575-0305.106. [DOI:10.16966/2575-0305.106] [PMID]

Tsuruoka, Y., Nakajima, T., Kanda, M., Hayashi, H., Matsushima, Y., & Yoshikawa, S., et al. (2017). Simultaneous determination of amantadine, rimantadine, and memantine in processed products, chicken tissues, and eggs by liquid chromatography with tandem mass spectrometry. *Journal of Chromatography. B, Analytical Technologies in The Biomedical and Life Sciences, 1044-1045,* 142–148. [DOI:10.1016/j.jchromb.2017.01.014] [PMID]

VasfiMarandi, M., Bozorgmehri Fard, M.H. (2002) Isolation of H9N2 Subtype of Avian Influenza Viruses during an Outbreak in Chickens in Iran. I*ranian Biomedical Journal 6*: 13-17. [Link]

Villegas, P. (2008) Titration of biological suspensions. *A laboratory manual for the isolation, identification, and characterization of avian pathogens.* Jacksonville: American Association of Avian Pathologists.

Watanabe, T., & Kawaoka, Y. (2015). Influenza virus-host interactomes as a basis for antiviral drug development. *Current Opinion in Virology, 14,* 71–78. [DOI:10.1016/j.coviro.2015.08.008] [PMID]

Waterhouse, A., Bertoni, M., Bienert, S., Studer, G., Tauriello, G., & Gumienny, R., et al. (2018). SWISS-MODEL: Homology modelling of protein structures and complexes. *Nucleic Acids Research, 46*(W1), W296–W303. [DOI:10.1093/nar/gky427] [PMID]

Yang, J., Li, M., Shen, X., & Liu, S. (2013). Influenza A virus entry inhibitors targeting the hemagglutinin. *Viruses, 5*(1), 352–373. [DOI:10.3390/v5010352] [PMID]

Yeaman, M. R., & Yount, N. Y. (2003). Mechanisms of antimicrobial peptide action and resistance. *Pharmacological Reviews, 55*(1), 27–55. [DOI:10.1124/pr.55.1.2] [PMID]

Zhao, H., To, K. K. W., Sze, K. H., Yung, T. T., Bian, M., & Lam, H., et al. (2020). A broad-spectrum virus-and host-targeting peptide against respiratory viruses including influenza virus and SARS-CoV-2. *Nature Communications, 11*(1), 4252. [DOI:10.1038/s41467-020-17986-9] [PMID]

Zhao, H., Zhou, J., Zhang, K., Chu, H., Liu, D., & Poon, V. K., et al. (2016). A novel peptide with potent and broad-spectrum antiviral activities against multiple respiratory viruses. *Scientific Reports, 6,* 22008. [DOI:10.1038/srep22008] [PMID]

مقاله پژوهشی

اثر بازدارندگی cLF-chimera، یک پپتید ضدمیکروب نوترکیب، بر ویروس آنفولانزای پرندگان، تحت تیپ H9N2

معین خدایاری[1]، محمد هادی سخاوتی[2]، سید مصطفی پیغمبری[1]، عباس برین[3]، امید دزفولیان[4]، جمشید رزمیار[1]

۱. گروه بیماریهای پرندگان، دانشکده دامپزشکی، دانشگاه تهران، تهران، ایران.

۲. گروه علوم دامی، دانشکده کشاورزی، دانشگاه فردوسی مشهد، مشهد، ایران.

۳. گروه آسیب شناسی بالینی، دانشکده دامپزشکی، دانشگاه تهران، تهران، ایران.

۴. گروه پاتوبیولوژی، دانشکده دامپزشکی، دانشگاه لرستان، خرم آباد، ایران.

چکیده

زمینه مطالعه: ویروس آنفولانزای پرندگان تحت تیپ H9N2 شایع‌ترین تحت تیپ ویروس آنفولانزا در ماکیان سراسر جهان است. این تحت تیپ باعث ایجاد ضررهای اقتصادی به صنعت پرورش ماکیان شده و قابلیت سرایت به انسان را دارد. در حال حاضر ۲ گروه عمده داروهای ضدآنفولانزا یعنی آدامانتان‌ها و مهار کننده‌های نورآمینیداز برای درمان این تحت تیپ در حال استفاده هستند. پپتیدهای ضدمیکروب که در سالیان اخیر استفاده از آن‌ها به دلیل مقاومت نسبت به داروهای ضدآنفولانزا رو به افزایش بوده‌است، دسته‌ای از ترکیبات کاندید احتمالی برای درمان آنفولانزا با طیف اثر وسیع هستند. cLF-chimera یک پپتید ضدمیکروب است که از لاکتوفرین شیر شتر سنتز شده‌است.

هدف: هدف این مطالعه بررسی اثرات بازدارندگی cLF-chimera بر روی تحت تیپ H9N2 ویروس آنفولانزای پرندگان می‌باشد.

روش کار: برای این منظور ۱۷۰ عدد تخم‌مرغ جنین‌دار ۱۱ روزه SPF به طور تصادفی در ۱۷ گروه توزیع شدند. غلظت‌های مختلف پپتید و ویروس به تخم‌مرغها تزریق شده و تخم‌مرغ‌ها به مدت ۴ روزهمراه با کندلینگ روزانه به منظور بررسی میزان زنده‌مانی جنین‌ها انکوبه شدند. در روز چهارم، جنین‌های زنده و مرده در هر گروه جدا شده و از لحاظ وجود ضایعات ماکروسکوپیک ارزیابی شدند. سپس برای مطالعات هیستوپاتولوژیک، جنین‌ها به مدت یک هفته در فرمالین ۱۰٪ نگهداری شدند. همچنین تست MTT هم برای غلظت‌های مختلف ویروس و پپتید انجام شد.

نتایج: روی هم رفته نتایج مربوط به درصد زنده‌مانی جنین‌ها، ارزیابی‌های ماکروسکوپیک و هیستوپاتولوژیک نشان دادند که پپتید دارای اثرات بازدارندگی علیه ویروس می‌باشد. این نتایج با نتایج حاصل از تست MTT تاییدشدند. علاوه‌براین، پپتید دارای اثرات ضدمیکروبی علیه باکتری‌های پاتوژن می‌باشد که در مقایسه با داروهای ضدآنفولانزای رایج می‌تواند به عنوان یک مزیت درنظر گرفته‌شود.

نتیجه‌گیری نهایی: طبق نتایج ذکرشده، cLF-chimea دارای اثر بازدارندگی علیه ویروس آنفولانزای تحت تیپ H9N2 می‌باشد.

کلیدواژه‌ها: آنفولانزای پرندگان؛ پپتید ضدمیکروب؛ تحت تیپ H9N2؛ هیستوپاتولوژی؛ cLF-chimera

٭ **نویسنده مسئول:**

دکتر جمشید رزمیار

نشانی: تهران، دانشگاه تهران، دانشکده دامپزشکی، گروه بیماریهای پرندگان.

رایانامه: jrazmyar@ut.ac.ir

This Page Intentionally Left Blank